International Journal of Environmental Sciences
ISSN: 2229-7359
Vol. 11 No. 6S, 2025
https://www.theaspd.com/ijes.php

Modelling, Thermal Analysis and Optimization of Phase Change Material based Heat Sink with Oblique Porous Copper Fins.

Gokul Depuk T.P[1], Sunil Chandel[2], Suresh Srivastava[3]
[1]CABS, DRDO
Bangalore-560037
[2]DIAT, DRDO
Pune- 411025
[3]CABS, DRDO
Bangalore- 560037

Abstract: This research focuses on the modelling, thermal analysis, and optimization of a phase change material (PCM) based heat sink with oblique porous copper fins. The study aims to address the challenge of heat dissipation in high-performance electronic devices by exploring the use of PCM, specifically RT50 and RT60, integrated with oblique porous copper fins. The research employs both 3D and 2D modelling techniques, utilizing ANSYS software for simulation. The 2D simulations, representing different oblique models with varying fin and PCM lengths, are developed to analyze heat transfer through fins and convection on the air surface. The study considers the material properties of PCM, including RT50, RT60, and thermal conductivity enhancers (TCE) such as copper. Meshing, boundary conditions, and natural convection are essential aspects of the methodology. The results of numerical simulations reveal the temperature profile and liquid fraction during the melting and solidification phases for both RT50 and RT60 under adiabatic and natural convection conditions. The findings emphasize the significance of RT60 in expediting melting and solidification phenomena, providing valuable insights for designing efficient PCM-based heat sinks.

Keywords: Phase Change Material, Heat Sink, Thermal Analysis, Porous Copper Fins, Numerical Simulation.

1. INTRODUCTION

Heat sinks are passive cooling mechanisms designed to dissipate heat from electronic or mechanical components like CPUs, GPUs, and power transistors. Heat dissipation is a major challenge in the development of high-performance and miniaturized electronic devices, as traditional air cooling methods are insufficient for high-density heat dissipation (Ahmed et al., 2018). A heat sink absorbs and transfers thermal energy away from electronic components to reduce heat accumulation and improve operational efficiency and reliability. Inefficient heat removal from the heat sink can lead to temperature rise and potential damage to electronic components. Heat sinks are usually made of aluminium or copper. These heat sinks often have fins, grooves, or other features to increase their surface area. (Rath et al., 2021)

A heat sink absorbs thermal energy produced by electronic components during operation. This heat is transferred to the heat sink by direct contact or thermal interface material (Kumar et al., 2021). The heat sink then evenly distributes the assimilated thermal energy throughout its surface using its excellent thermal conductivity (Zhang & Wang, 2019). The research article focuses on the design of thermal management systems to prevent overheating and failure of electronic components due to high power density (Kumar et al., 2020). The study numerically investigates the thermal performance of heat sink configurations with different numbers of cavities (ranging from 1 to 36) formed by cross plate fins arrangement. Increased surface area aids heat dissipation, where the heat sink rises in temperature and releases thermal energy into the atmosphere. Different types of pin fin geometries, such as hexagonal, circular, rhombus, and perforated pin fins, are analysed to compare their heat transfer performance and fluid flow behaviour (Bhandari & Prajapati, 2021). Airflow, whether natural or induced by fans, removes heat from a system or object. The paper provides a comprehensive overview of thermal heat

sink design and optimization, discussing heat transfer enhancement strategies, fin design trends, and different fin configurations (Gaikwad et al., 2023).

2. LITERATURE REVIEW

Heat sinks vary in shape and size depending on the application and heat dissipation needed. These components are found in computers, laptops, electronics, industrial, and automotive applications (Zhang et al., 2012). In this study, experiments are conducted to measure the thermal resistances of heat sinks with cross-cut branched fins on horizontal cylinders. The paper discusses the design of an aluminum alloy heat sink for cooling a PCB with specific dimensions and power dissipation, using forced convection with a cooling fan (Reddy, 2015). The experiments were conducted for several numbers of fin, heights of fins, and heat inputs (Kim & Kim, 2021). Phase Change Material (PCM) heat sinks are advanced thermal management solutions designed to distribute electronic component heat. Phase shift materials in the heat sinks can transform from solid to liquid at a set temperature (Husainy et al., 2023). The study investigates the thermal behaviour of a PCM-based heat sink with horizontal fins in electronic cooling applications. The objective is to maximize the safe operation time by optimizing the number of fins(Rostami et al., 2020).

Phase Change Material (PCM)-based heat sinks are ideal for maintaining a consistent temperature since they can give a stable temperature range. Thermal management benefits from PCM-based heat sinks (Ho et al., 2021). The authors conducted experiments to evaluate the heat dissipation capabilities of the PCM-based heat sink and found that it provided better thermal performance compared to the conventional design. The study focuses on enhancing the charging rate and uniformity of the melting rate in phase change material (PCM)-based thermal energy storage units (TESU) by using asymmetric fins (Shaban et al., 2023). They enable passive cooling, reduce temperature swings, improve thermal performance, and reduce the demand for fans. The paper discusses the use of phase change materials (PCMs) as a solution for thermal management in compact electronic devices. It explores different types of PCMs and their efficiency and implementation parameters. It also mentions the use of internal fins, nanomaterials, and metal foams as thermal conductivity enhancers (Khan, 2022). To achieve the best results, the phase change material (PCM) and temperature must be carefully selected for the application. By arranging parallel PCBs to form a channel and optimizing cooling airflow rates, the thermal resistance is reduced by 30% compared to previous designs. The orientation effect on the channel design is found to be 10% less than the reference design, and the LED bulb's lifespan is shown to be 40% longer than existing geometries (Jang et al., 2015). The use of porous materials in MCHS, such as porous fins and porous substrates, has been investigated to reduce pressure drop and enhance heat transfer capability (Bagherighajari et al., 2022). The study uses numerical methods and an orthogonal experimental method to analyse the thermal influences of structure parameters on the heat sink and shows that the designed heat sink significantly reduces the working temperature of the propeller driver (Lai et al., 2023). Dispersing electronic component heat with a phase change material (PCM) and copper-finned heat sink is a specialised thermal management approach. This design improves heat dissipation by combining phase change materials (PCM) with oblique copper fins. Oblique fins enhance effective surface area, produce turbulent airflow, and reduce air resistance. This research investigates the finite element volume characterization study by utilization of phase change materials (PCMs) within heat sinks for the purpose of controlling the temperature of electronic devices. Specifically, it explores the application of non-homogeneous porous copper metal foams as enhancers of thermal conductivity, in conjunction with paraffin as the phase transition material.

3. METHOD AND METHODOLOGY

3.1 3D and 2D modelling of PCM

The 3D model, created using ANSYS, features a heat sink with dimensions of 62mm in length and 120mm in width, a Copper foam fin with an 18.25:1.75 ratio, and an air gap of 2mm.

The 3D model, designed in ANSYS, consists of a heat sink with precise dimensions of 62mm in length

and 120mm in width, tailored for efficient heat dissipation. The model incorporates copper foam fins, structured with a specific aspect ratio of 18.25:1.75 to optimize thermal conductivity and heat transfer. Additionally, a 2mm air gap has been included strategically between the components to prevent the phase change material (PCM) from overflowing upon melting, enhancing both stability and performance in thermal management. This setup is critical for simulating realistic conditions under varying heat loads and for evaluating the model's effectiveness in passive cooling applications.

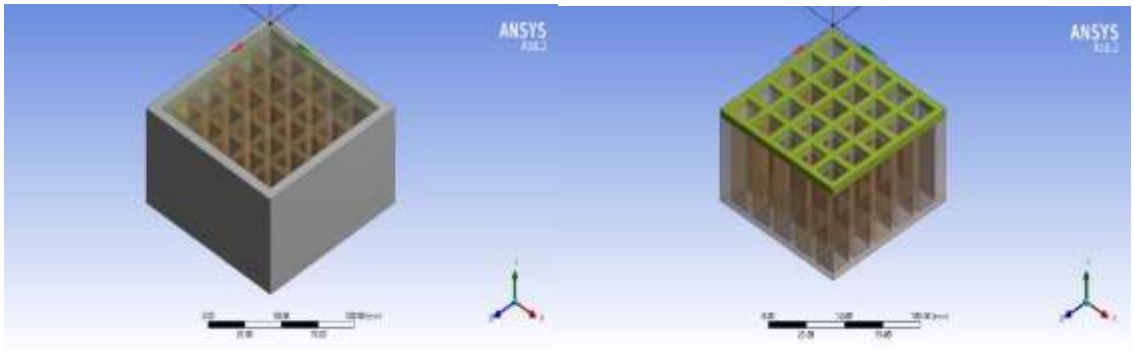

Fig.1.a) Isometric View of 3D PCM and **Fig.1.b)** Air Gap in PCM

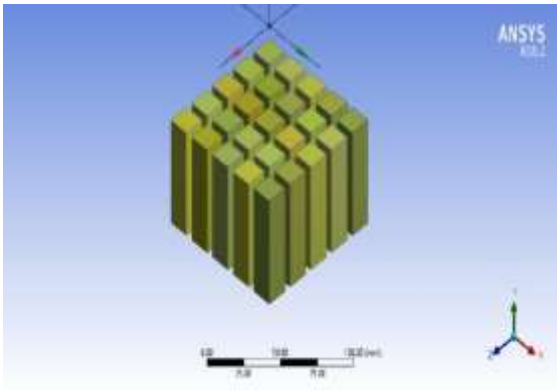

Fig.1.c) Fins in PCM

A 2D simulation of a 3D model yields accurate results with minimal computational time, compared to 3D simulations. A 2D design of the same model is developed, creating seven oblique models with different fin and PCM lengths. Design changes affect heat transfer through fins and convection via top air surface. An air gap is created to prevent molten PCM overflow.

Model 1 : Fin length top - 1.25, bottom - 18.75

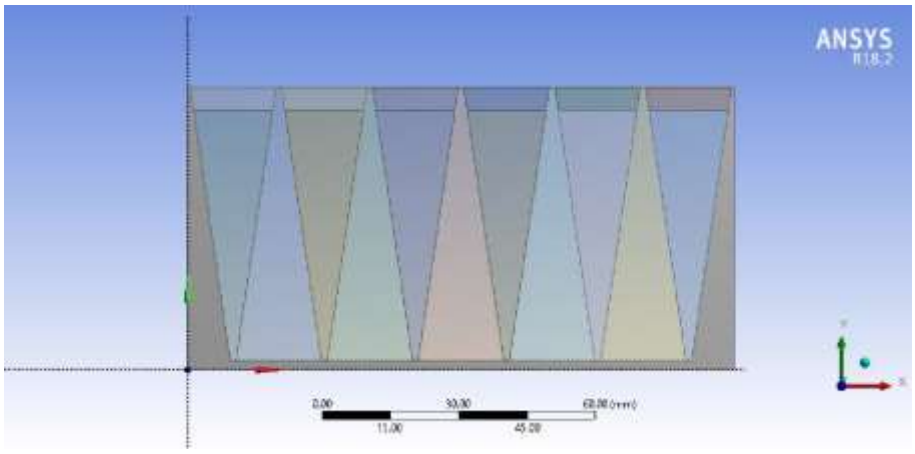

Fig.2. 2D model of PCM

3.2 Material Properties

To improve thermal conductivity, Thermal Conductivity Enhancers (TCE) are used, with solid materials like copper and liquid materials like RT50 and RT60 analysed.

Table 1: Material Properties of PCM

Material	Density ρ(Kg/m^3)	Specific heat capacity Cp(J/Kg K)	Thermal conductivity K(W/mK)	Dynamic Viscosity μ (PA s)	Latent heat L(kJ/kg)	Thermal expansion coefficient (1/k)	Melting temperature Range K
RT50	800	1800	0.2	0.002	250	0.007	45-55
RT60	805	2660	0.2	0.0003	110	0.0007	53-61
Copper	8993	380	400	-	-	-	-

3.3 Meshing

Meshing is crucial in fluent simulation, with face and size meshing in model faces and edges. Medium mesh density is used, as fine mesh increases computational time.

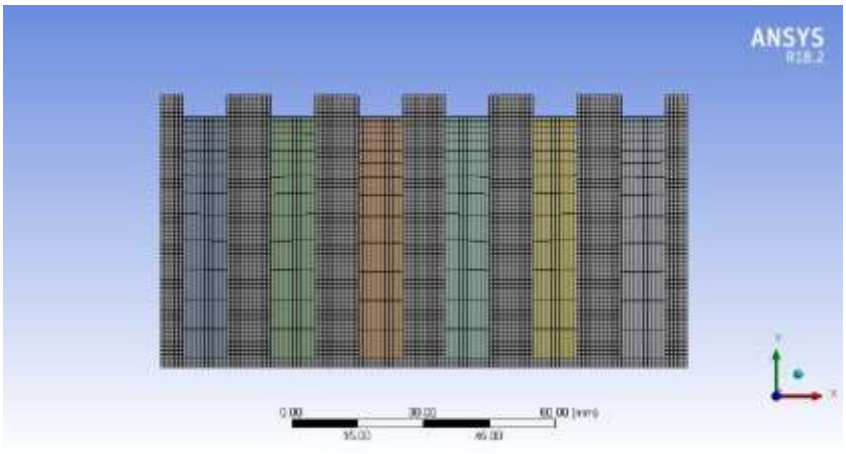

Fig.3. Meshing of PCM

The finite element mesh appears to be created likely in the ANSYS R18.2 software package. It appears that it is a 2D mesh, because no third dimension can be found in the mesh. It looks like a meshing strategy with quadrilateral elements has been used; the quadrilateral element is preferable when better numerical stability and accuracy can be expected over the triangular element in many cases. The elements are mainly uniform in size, indicating a structured meshing technique. Uniformity helps in better numerical behavior and leads to faster convergence of the solution.

The mesh density seems to be quite uniform over the domain, with no drastic variations in the element size. Uniformity is critical for an accurate representation of the physical phenomenon under study. But again, without specific context on the type of analysis being carried out (stress, fluid flow), the mesh density will likely be too sparse to give meaningful results. As a rule, mesh resolution needs to increase in areas that have localized behavior, such as stress concentrations and rapid changes in fluid flow.

While the image provides a visual representation of the mesh, a more comprehensive assessment of mesh quality would require examination of numerical metrics such as element aspect ratios, skewness, and Jacobian values. These metrics provide quantitative measures of element shape and quality, which directly impact the accuracy and convergence of the finite element solution.

3.4 Boundary Condition

The initial loading condition for the model is 300K, with natural convection set on the left, right, and top edges, and adiabatic conditions on the left and right sides. A transient heat flux is applied to the bottom edge due to contact with the heat source.

It represents a finite element mesh generated using the ANSYS environment. The mesh is probably meant for numerical analysis, such as structural analysis, fluid dynamics, or heat transfer. The discretization of geometry into smaller parts through the process of meshing allows for numerical simulation of very complex physical phenomena.

Boundary Conditions are essentially the conditions that describe the interaction between the model and its surround. It is a statement of all applied physical constraints and loads at the boundaries of the model. For this context, boundary conditions will describe the conditions on the meshed domain boundaries.

Some possible Boundary Conditions that could be set for this model are:

Fixed Supports: These simulate constraints like a model clamped or affixed to a rigid surface. They can be thought of as nodes on the boundary which are constrained to not displace in a specific direction, say in x direction.

Applied loads applied to simulate such forces or pressure which may either be in fluid pressures, loads or thermal as per the demand. These demands are applied within the appropriate bounds in the following manners: The symmetry/ anti-symmetry. This entails taking advantage of symmetry or antisymmetry. Here, if symmetry or antisymmetry presents itself in terms of geometry together with loading cases, then less computing is to be done at the boundary constraint is applied correctly.

Thermal Loads: To account for temperature variations or heat fluxes applied on model boundaries like convection and/or radiative heat exchange.

Again, the exact conditions would be case-specific in order to get correct results depending upon the analysis desired. For these boundary conditions too, precise determination and imposition shall ensure an excellent numerical approximation to the realistic phenomena of the underlying system being under study.

3.5 Natural convection

Natural convection is a fundamental phenomenon within the field of fluid dynamics and heat transfer. It is primarily driven by buoyant forces resulting from temperature gradients, and it holds considerable importance in a wide range of both natural and engineered processes.

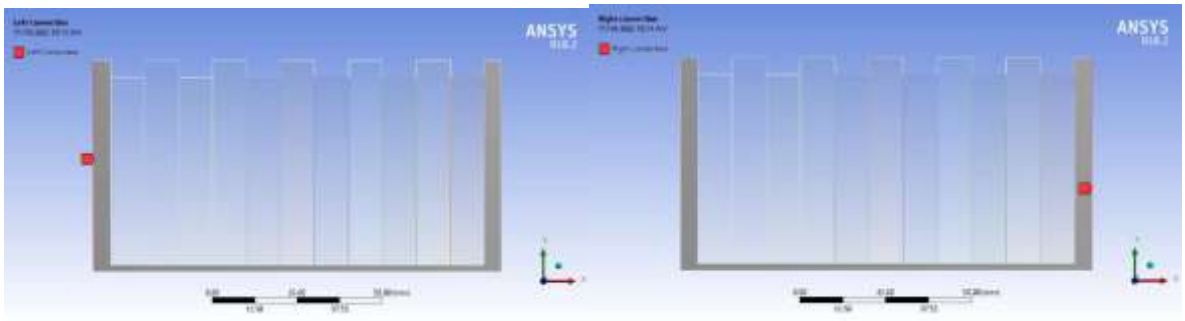

International Journal of Environmental Sciences
ISSN: 2229-7359
Vol. 11 No. 6S, 2025
https://www.theaspd.com/ijes.php

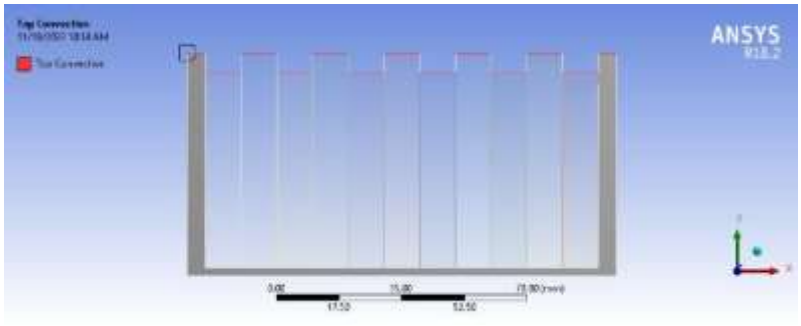

Fig. 4 Natural convection

3.6 Heat flux : Connected to the Heat Source

The concept of heat flux pertains to the quantification of heat energy transfer per unit area, hence denoting the magnitude of heat energy traversing a certain surface or medium within a specified time interval.

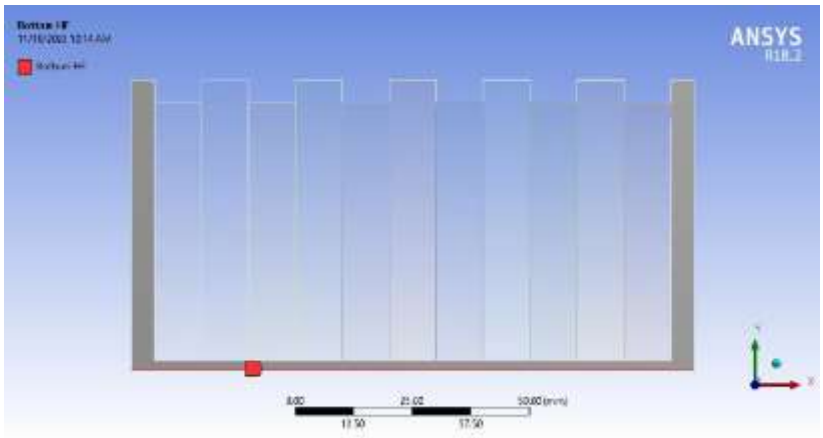

Fig. 5 Connected to the Heat Source.

3.7 Convergence study

A convergence study refers to a methodical analysis or inquiry carried out in numerical simulations and computational modelling to assess the accuracy of a numerical solution in approximating the true or desired solution as the computational parameters undergo refinement or alteration. The study used a simulation model consisting of five meshes in order to investigate the effects of grid dependency, computing time, and accuracy. The PISO scheme and PRESTO! approach is commonly employed in the context of pressure-velocity coupling and spatial discretization. The selection of Model 3, which possesses an intermediate mesh density, is justified for subsequent simulations as it is compatible with all 15 models.

4. SIMULATION RESULTS

4.1 Numerical Simulations

The present study involves the utilization of numerical simulations to investigate the behaviour of two distinct phase change materials, namely RT50 and RT60. The simulations are conducted under a controlled experimental condition, where a continuous heat flux of 5 kW/m^2 is applied for a duration of 3000 seconds. The charging process commences with a consistent heat flow, whereas the discharge process commences with a lack of heat flux. The procedure encompasses six distinct stages, namely pre-sensible heating, phase change, and discharge. The baseline temperature remains consistent, while the rate of temperature decrease is accelerated during the solidification of the phase change material (PCM).

The rate of heat transfer is directly proportional to the temperature of the heat sink, resulting in a deceleration of the cooling process as the heat sink temperature lowers.

In a system that is adiabatic, there is an absence of heat transfer between the system and its surroundings, leading to a comparatively consistent distribution of temperature. The fluctuations in temperature typically arise from negligible beginning circumstances or mistakes in measurement. On the other hand, natural convection, which is propelled by disparities in temperature, can have a substantial temperature profile. The temperature distribution is influenced by various elements, including the geometric characteristics of the system, the temperature disparity between the object and its surrounding environment, and the qualities of the fluid medium. The temperature distribution is influenced by the flow patterns generated through natural convection. The temperature profiles in all scenarios are contingent upon the particular parameters of the system. When comparing the temperature profiles of two distinct phase change materials under adiabatic and natural convection settings, it is seen that the adiabatic condition yields greater temperature values compared to the boundary conditions of natural convection.

4.2 Temperature Profile

Results are formulated for temperature profile for both adiabatic and natural convection for two phase change materials RT50 and RT60.

The relationship between charging time and melting temperature in a phase change material (PCM) heat sink is complex and depends on several factors. The choice of PCM material, initial temperature difference, heat source, heat transfer mechanism, heat sink design, control systems, and phase change temperature range all influence the charging time. Higher melting temperatures generally require more time and energy to melt, while larger temperature differences result in faster charging. The efficiency of heat transfer to the PCM is critical, and the design of the heat sink can impact the rate of heat transfer and charging time.

For all models in adiabatic condition and natural convection for RT 50 PCM, it is found that charging time increases the melting point of the phase change material is observed in temperature profile. For all models, Comparing temperature profiles for the adiabatic and natural convection for two different phase change material, the adiabatic condition results in higher temperature values than the natural convection boundary conditions.

4.3 Different results analysed for various conditions with respect to RT 50 and RT 60:

4.3.1 Adiabatic condition RT 50

Table 2: Adiabatic measure for varying time for all the models considered

Time	MODEL-1	MODEL-2	MODEL-4	MODEL-5	MODEL-6	MODEL-7
	1-Adi - RT50	2-Adi - RT50 -	4-Adi - RT50 -	5-Adi - RT50 -	6-Adi - RT50	7-Adi - RT50 -
0	300.00	300.00	300.00	300.00	300.00	300.00
1000	321.11	321.05	320.89	320.83	320.72	320.68
1500	323.87	323.68	323.31	323.18	323.00	322.90
2000	326.26	326.03	325.47	325.29	325.04	324.89
2500	327.50	327.47	327.21	327.05	326.78	326.53
3000	327.88	327.82	327.65	327.77	327.88	328.39

The table 2 presents the evolution of the RT50 values (probably representing a response time or some similar performance metric) for seven different models ranging from MODEL-1 to MODEL-7 over 3000 seconds. All the models, at time 0, start with the same RT50 value of 300.00. In different models, at various points of time, their RT50 values take different shapes and forms. Some of the models depict

a constant rise in RT50 (such as MODEL-7), while others display stable behavior with less fluctuation (like MODEL-4 and MODEL-5). The table above thus depicts the dynamic behavior of these models and the changing performance metrics over time.

4.3.2 Natural convection RT 50

Table 3: Natural convection for varying time for all the models considered

Time	MODEL-1	MODEL-2	MODEL-4	MODEL-5	MODEL-6	MODEL -7
	1-NC - RT50	2-NC-RT50 -	4-NC-RT50	5-NC-RT50 -	6-NC-RT50 -	7-NC-RT50 -
0	300.00	300.00	300.00	300.00	300.00	300.00
500	317.07	317.17	317.19	317.10	316.88	316.67
1000	320.56	320.51	320.39	320.32	320.23	320.17
1500	322.97	322.81	322.49	322.37	322.20	322.10
2000	325.13	324.90	324.40	324.23	324.00	323.84
2500	326.61	326.51	326.04	325.85	325.61	325.44
3000	327.79	327.79	327.51	327.36	327.04	326.77

The table describes the development of RT50 values (most likely, response time or any similar performance parameter) for seven models from MODEL-1 to MODEL-7 with respect to a duration of 3000 seconds at a natural convection environment. In the beginning at time zero (0), the value of RT50 for all the models is 300.00. While progressing with the time, different models of RT50 show divergent behavior. For example, some models, like MODEL-1, MODEL-2, and MODEL-3, show a progressive increase in RT50 over time. Other models, such as MODEL-4, MODEL-5, and MODEL-6, have relatively stable behavior with minimal variations in their RT50 values. MODEL-7, on the other hand, has a consistent increase in RT50 over the entire observation period. These differences in RT50 values among different models may indicate variations in their thermal behavior or response characteristics under natural convection conditions. Further analysis would be required to understand the factors that might cause these trends and their implications on the performance of these models.

4.3.3 Adiabatic condition RT 60

Table 4: Adiabatic measure for varying time for all the models considered

Time 1 -	MODEL - 1	MODEL - 2	MODEL - 3	MODEL - 4	MODEL - 5	MODEL - 6	MODEL - 7
	Adi - RT60 2 -	- Adi - RT60 3 -	Adi - RT60 4 -	Adi - RT60 5	- Adi - RT60 6	- Adi - RT60	7 - Adi - RT60
0	300.00	300.00	300.00	300.00	300.00	300.00	300.00
500	315.77	315.63	315.40	315.24	315.07	314.81	314.65
1000	327.02	327.02	327.00	326.96	326.86	326.63	326.46
1500	331.39	331.17	330.86	330.67	330.49	330.23	330.07
2000	333.21	333.15	333.06	333.03	332.97	332.77	332.49
2500	333.99	333.91	333.87	333.83	333.72	333.81	333.89
3000	333.99	333.91	333.87	333.81	333.72	333.75	333.79

The table shows the time evolution of RT60 values, probably reverberation time, for seven different models, MODEL-1 to MODEL-7, over a period of 3000 seconds. At the initial time, 0 seconds, all models have the same RT60 value of 300.00. As time progresses, the RT60 values for different models show different trends. Some models, such as MODEL-1, MODEL-2, and MODEL-3, show a gradual increase in RT60 over time. On the other hand, MODEL-4, MODEL-5, and MODEL-6 are rather stable in the variations of RT60. For MODEL-7, it reveals a continuous trend of increasing values of RT60 over the time of observation. Such changes of RT60 from one model to another might suggest some difference in acoustic properties or even in the responses of these models. Further analysis would be needed to understand the underlying factors behind these observed trends and their implications for the acoustic performance of these models.

4.3.4 Natural convection RT 60

Table 5: Natural convection for varying time for all the models considered

Time	MODEL - 1	MODEL - 2	MODEL – 3	MODEL - 4	MODEL - 5	MODEL - 6	MODEL - 7
	1 - NC- RT60	2 - NC - RT60	3 - NC - RT60	4 - NC - RT60	5 - NC - RT60	6 - NC - RT60	7 - NC - RT60
0	300.00	300.00	300.00	300.00	300.00	300.00	300.00
500	315.05	314.93	314.73	314.58	314.42	314.18	314.02
1000	326.03	326.05	326.04	325.97	325.85	325.58	325.36
1500	329.88	329.72	329.49	329.34	329.19	328.96	328.83
2000	332.48	332.39	332.15	331.95	331.73	331.42	331.20
2500	333.49	333.46	333.47	333.46	333.39	333.13	332.86
3000	333.85	333.80	333.76	333.72	333.63	333.66	333.73

The table shows the development of RT60 values, which are probably reverberation time, for seven different models, MODEL-1 to MODEL-7, for a duration of 3000 seconds under No-Coupling (NC) conditions. All the models show the same value of RT60 at the beginning time, 0 seconds, as 300.00. With the progression of time, the RT60 values for different models show varied behavior. Some models, like MODEL-1, MODEL-2, and MODEL-3, present a gradual increase in RT60 over time. On the other hand, models such as MODEL-4, MODEL-5, and MODEL-6 tend to be stable with minimal fluctuations in their RT60 values. MODEL-7 presents a steadily increasing RT60 throughout the observation period. Such variations in RT60 values of different models might indicate differences in their acoustic properties or response characteristics under No-Coupling conditions. Further analysis would then be required in order to appreciate the underlying drivers of these observed trends and how they impact on the acoustic performance of these models.

4.3.5 Temperature Profile

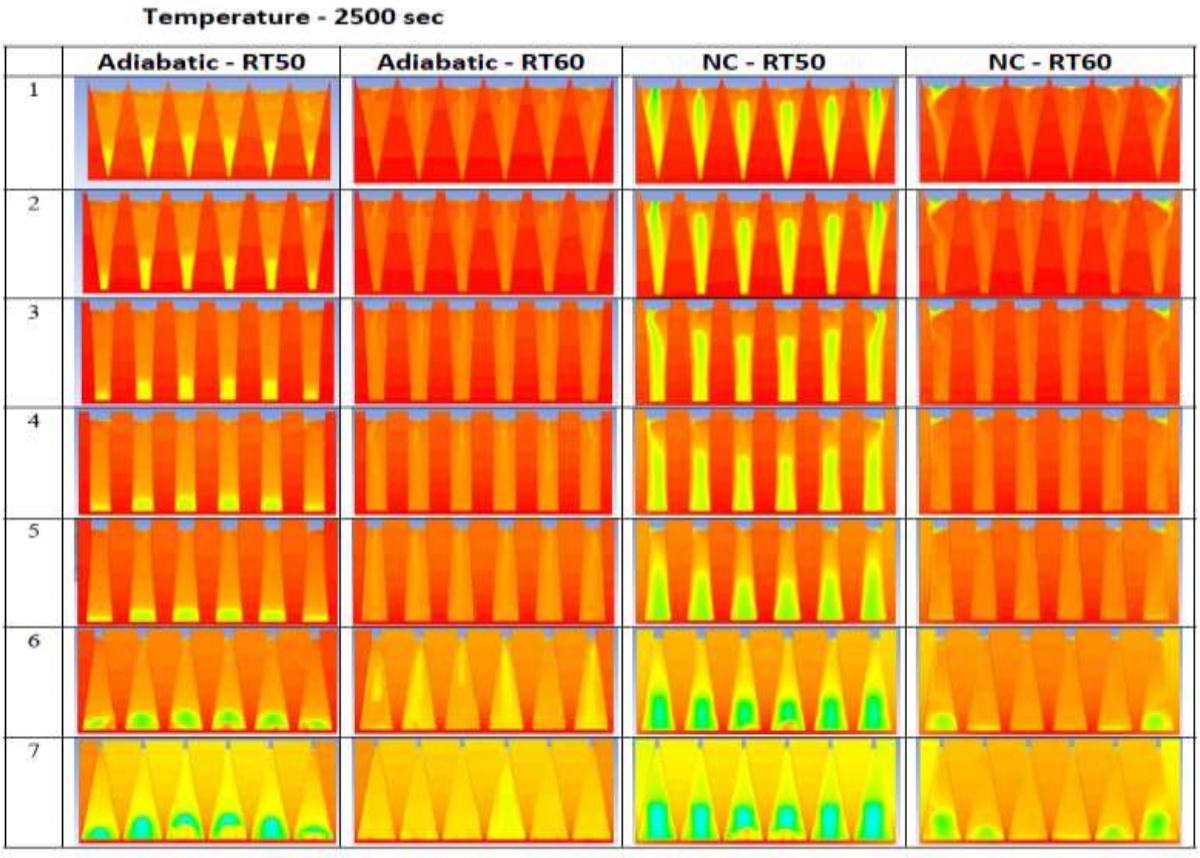

Figure 6: Temperature profile for both Adiabatic and Natural Convection in RT 50 and RT 60

4.4 Liquid Fraction profile for RT 50 and RT 60

The liquid fraction profile is a valuable analytical tool that provides insights into the temporal or spatial variations in the amount of liquid within a given sample. Phase change materials (PCMs) and other systems that undergo transitions between solid and liquid states frequently employ this particular substance. The profile has three distinct zones, namely solid, transition, and liquid. The solid zone refers to the portion of the material that is completely solid, whereas the transition region denotes the area where the substance is wholly in a liquid state.

In an adiabatic system, the material's initial state is characterized by its solid phase below the melting point. Heating is facilitated by internal heat, leading to an increase in temperature that approaches the melting point. As the temperature increases, the solid undergoes a phase change, resulting in pockets of liquid. The expansion of the liquid phase occurs with the introduction of more thermal energy, leading to an increase in the proportion of the liquid fraction. This process persists until the entire material attains the ultimate melting temperature.

The solidification process begins when the substance is completely liquid, beyond its melting temperature. The cooling process occurs due to thermal energy dissipation, leading to a decrease in temperature below the material's melting point. This leads to the generation of solid nuclei, which increase in size as the temperature decreases. As the solid phase grows, the liquid phase experiences a reduction in size, resulting in a fall in the liquid fraction. The process persists until the entire material reaches the ultimate melting temperature.

Natural convection is a heat transfer mechanism that involves the movement of a fluid due to density differences caused by temperature variations. It helps maintain controlled and stable temperatures

within the system. Adiabatic systems lack heat exchange with the surroundings, leading to internal energy changes and significant temperature changes, especially during phase change processes like melting or solidification.

4.4.1 Liquid fraction - Melting - Adiabatic RT50

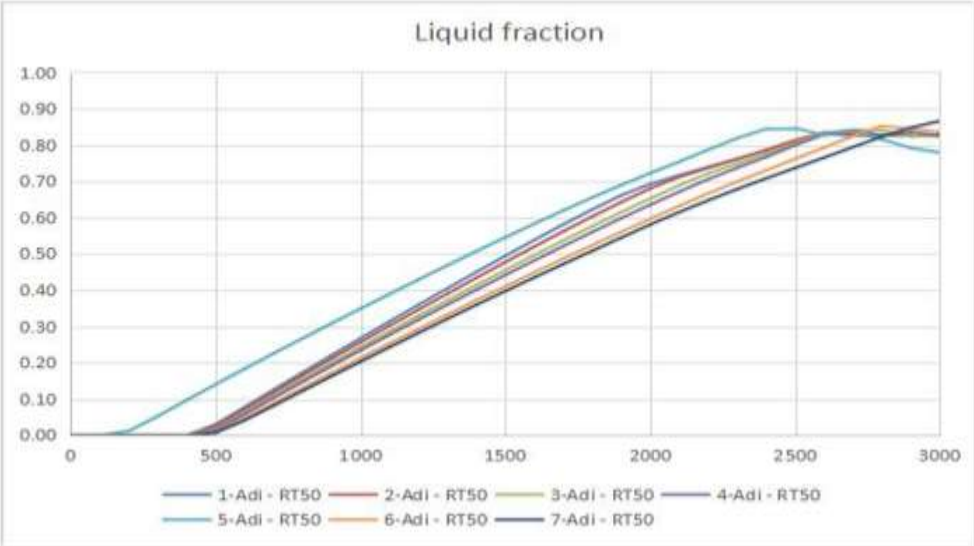

Figure 7: Liquid fraction for Melting -Adiabatic RT 50

Table 6: Liquid fraction for varying time for all the models considered under adiabatic condition RT50

Time	MODEL - 1	MODEL - 2	MODEL – 3	MODEL - 4	MODEL - 5	MODEL - 6	MODEL - 7
	1 - Adi-RT50	2 - Adi - RT50	3 - Adi - RT50	4 - Adi - RT50	5 - Adi - RT50	6 - Adi - RT50	7 - Adi - RT50
0	0.00	0.00	0.00	0.00	0.00	0.00	0.00
500	0.03	0.03	0.02	0.01	0.14	0.01	0.01
1000	0.27	0.26	0.24	0.23	0.35	0.21	0.20
1500	0.49	0.48	0.46	0.44	0.55	0.41	0.40
2000	0.69	0.68	0.65	0.64	0.72	0.60	0.58
2100	0.72	0.71	0.69	0.67	0.75	0.63	0.62
2200	0.74	0.74	0.72	0.71	0.79	0.67	0.65
2300	0.76	0.76	0.75	0.74	0.82	0.70	0.68
2400	0.79	0.79	0.78	0.77	0.84	0.73	0.71
2500	0.81	0.81	0.81	0.80	0.85	0.76	0.74
2600	0.83	0.83	0.83	0.83	0.83	0.79	0.77
2700	0.83	0.83	0.84	0.84	0.84	0.82	0.79
2800	0.83	0.83	0.84	0.83	0.82	0.85	0.82
2900	0.83	0.82	0.82	0.84	0.79	0.84	0.85
3000	0.83	0.83	0.82	0.83	0.78	0.84	0.87

The table shows the change in 1-Adi-RT50 values for seven different models, MODEL-1 to MODEL-7, over 3000 seconds. At time 0 seconds, all models have a 1-Adi-RT50 value of 0.00. As time passes, the 1-Adi-RT50 values of the different models vary. For example, the 1-Adi-RT50 values for MODEL-1, MODEL-2, and MODEL-3 increase with time but tend to level off at about 0.83. Others, such as MODEL-4 and MODEL-6, have a more oscillating pattern with an initial increase followed by a stable period. MODEL-5 has a large increase in 1-Adi-RT50 after 2000 seconds, while MODEL-7 has a slow

but steady increase throughout the observation period. These changes in 1-Adi-RT50 values among the models may indicate differences in their dynamic behavior or response characteristics. Further analysis would be required to understand the underlying factors contributing to these observed trends and their implications for the performance of these models.

4.4.2 Liquid fraction - Melting - Natural convection RT50

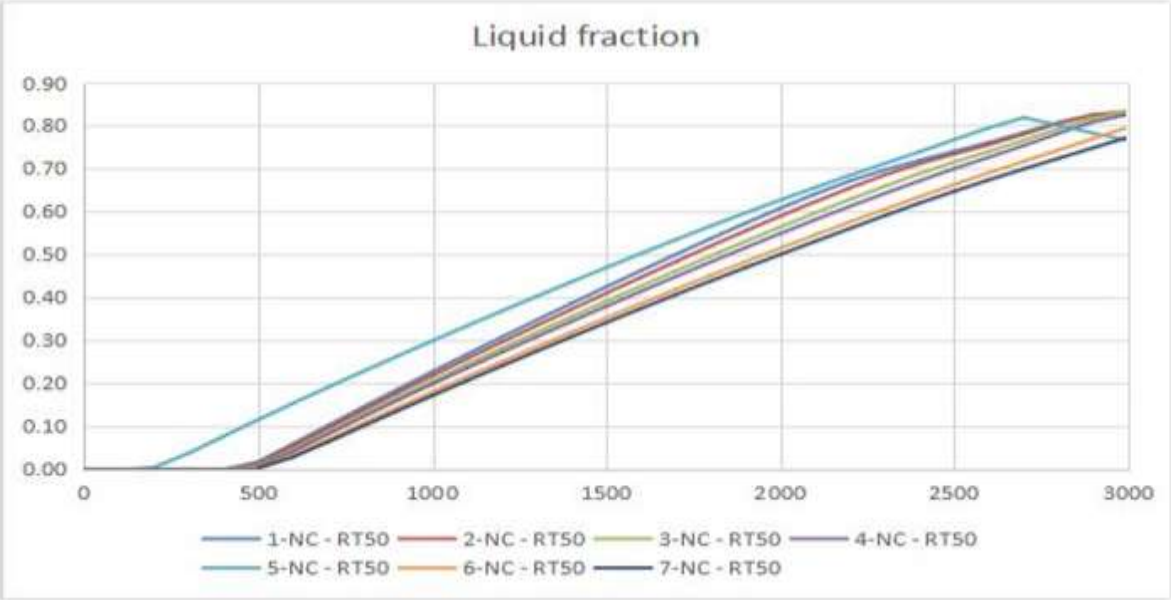

Figure 8: Liquid fraction for Melting -Natural Convection RT 50

Table 7: Liquid fraction for varying time for all the models considered under Natural Convection RT50

Time	MODEL - 1	MODEL - 2	MODEL – 3	MODEL - 4	MODEL - 5	MODEL - 6	MODEL – 7
	1 - NC - RT50	2 - NC - RT50	3 - NC - RT50	4 - NC - RT50	5 - NC - RT50	6 - NC - RT50	7 - NC - RT50
0	0.00	0.00	0.00	0.00	0.00	0.00	0.00
500	0.02	0.01	0.01	0.01	0.12	0.00	0.00
1000	0.23	0.22	0.21	0.20	0.30	0.18	0.17
1500	0.43	0.41	0.39	0.38	0.47	0.35	0.34
2000	0.61	0.59	0.56	0.55	0.63	0.52	0.50
2100	0.64	0.62	0.60	0.58	0.66	0.55	0.53
2200	0.67	0.66	0.63	0.61	0.68	0.58	0.56
2300	0.70	0.69	0.66	0.64	0.71	0.61	0.59
2400	0.72	0.71	0.69	0.67	0.74	0.63	0.62
2500	0.74	0.73	0.72	0.70	0.77	0.66	0.65
2600	0.76	0.76	0.74	0.73	0.80	0.69	0.67
2700	0.78	0.78	0.77	0.75	0.82	0.72	0.70
2800	0.81	0.81	0.79	0.78	0.80	0.74	0.72
2900	0.83	0.83	0.82	0.81	0.78	0.77	0.75
3000	0.83	0.83	0.83	0.83	0.77	0.80	0.77

The table depicts the time course of the 1-Adi-RT50 values for seven models: MODEL-1 to MODEL-7 from time 0 to 3000 seconds. All models present a 1-Adi-RT50 value of 0.00 at the starting time point

of 0 s. With passage of time, different models show various trends in their 1-Adi-RT50 values. Other models, including MODEL-1, MODEL-2, and MODEL-3, demonstrate a rather steady increase over time with regard to 1-Adi-RT50, peaking at about 0.83. Other models like MODEL-4 and MODEL-6 exhibit relatively wavering patterns of rising followed by levelling off. More interestingly, MODEL-5 exhibits a much more marked rise in 1-Adi-RT50 after 2000 seconds; MODEL-7, on the other hand, tends to be constantly rising with slight consistency. Interestingly, MODEL-5 and MODEL-7 both show a transitory peak in 1-Adi-RT50 around the 2500-second point, after which they stabilize or slightly decrease. These fluctuations in the 1-Adi-RT50 value among different models may indicate variations in their dynamic response or response characteristic. Further analysis is required to clarify the underlying cause of these observed trends and their significance for the performance of these models.

4.4.3 Liquid fraction - Melting - Adiabatic RT60

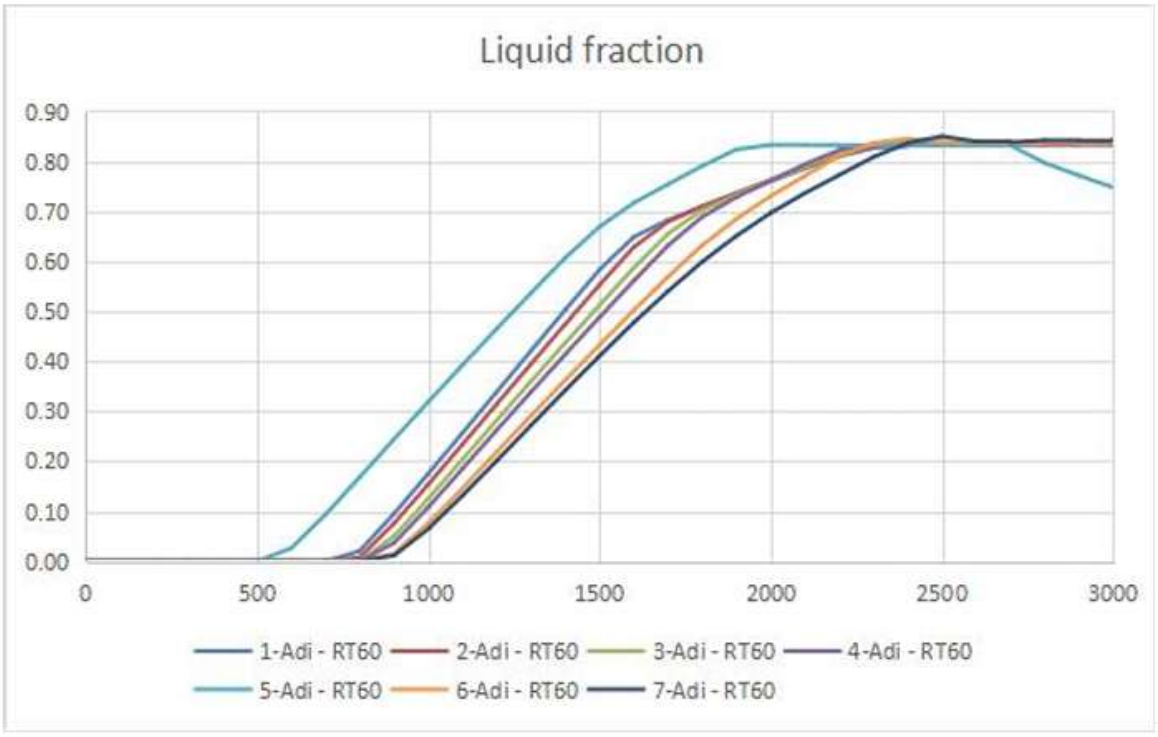

Figure 9: Liquid fraction for Melting -Adiabatic RT 60

Table 8: Liquid fraction for varying time for all the models considered under adiabatic condition RT60

Time	MODEL - 1	MODEL - 2	MODEL – 3	MODEL - 4	MODEL - 5	MODEL - 6	MODEL - 7
	1 - Adi-RT60	2 - Adi - RT60	3 - Adi - RT60	4 - Adi - RT60	5 - Adi - RT60	6 - Adi - RT60	7 - Adi - RT60
0	0.00	0.00	0.00	0.00	0.00	0.00	0.00
500	0.00	0.00	0.00	0.00	0.00	0.00	0.00
1000	0.18	0.15	0.13	0.11	0.32	0.08	0.06
1500	0.58	0.55	0.51	0.49	0.67	0.43	0.41
2000	0.76	0.76	0.76	0.76	0.83	0.73	0.70
2100	0.79	0.79	0.79	0.79	0.83	0.77	0.74
2200	0.81	0.81	0.82	0.82	0.83	0.81	0.77
2300	0.83	0.83	0.83	0.83	0.83	0.84	0.81
2400	0.83	0.83	0.84	0.84	0.83	0.85	0.84

2500	0.83	0.83	0.84	0.84	0.83	0.84	0.85
2600	0.83	0.83	0.84	0.83	0.83	0.84	0.84
2700	0.83	0.83	0.84	0.83	0.83	0.84	0.84
2800	0.83	0.83	0.84	0.83	0.80	0.84	0.84
2900	0.83	0.83	0.84	0.83	0.77	0.83	0.84
3000	0.83	0.83	0.84	0.83	0.75	0.84	0.84

Table gives the temporal variation of 1-Adi-RT60 values of seven models namely MODEL-1 to MODEL-7 within the time range of 3000 seconds. Starting from time (0 s) all the models have 1-Adi-RT60 value to be equal 0.00 and as the time increases the different models vary according to 1-Adi-RT60 values. Some models, like MODEL-1, MODEL-2, and MODEL-3, exhibit a steady increase in 1-Adi-RT60 over time, peaking at around 0.83. Others, such as MODEL-4 and MODEL-6, have a more oscillatory pattern with periods of increase followed by stability. MODEL-5 is interesting in that it has a very large increase in 1-Adi-RT60 after 2000 seconds, peaking at about 0.85. Interestingly, MODEL-5 and MODEL-7 present a transient peak in 1-Adi-RT60 values around the 2500-second mark, after which it stabilizes or slightly decreases. These fluctuations in 1-Adi-RT60 values among different models may indicate that their dynamic behavior or response characteristics are different from one another. Further analysis would be required to understand the factors behind these observed trends and how they impact the performance of the models.

4.4.4 Liquid fraction - Melting - Natural convection RT60

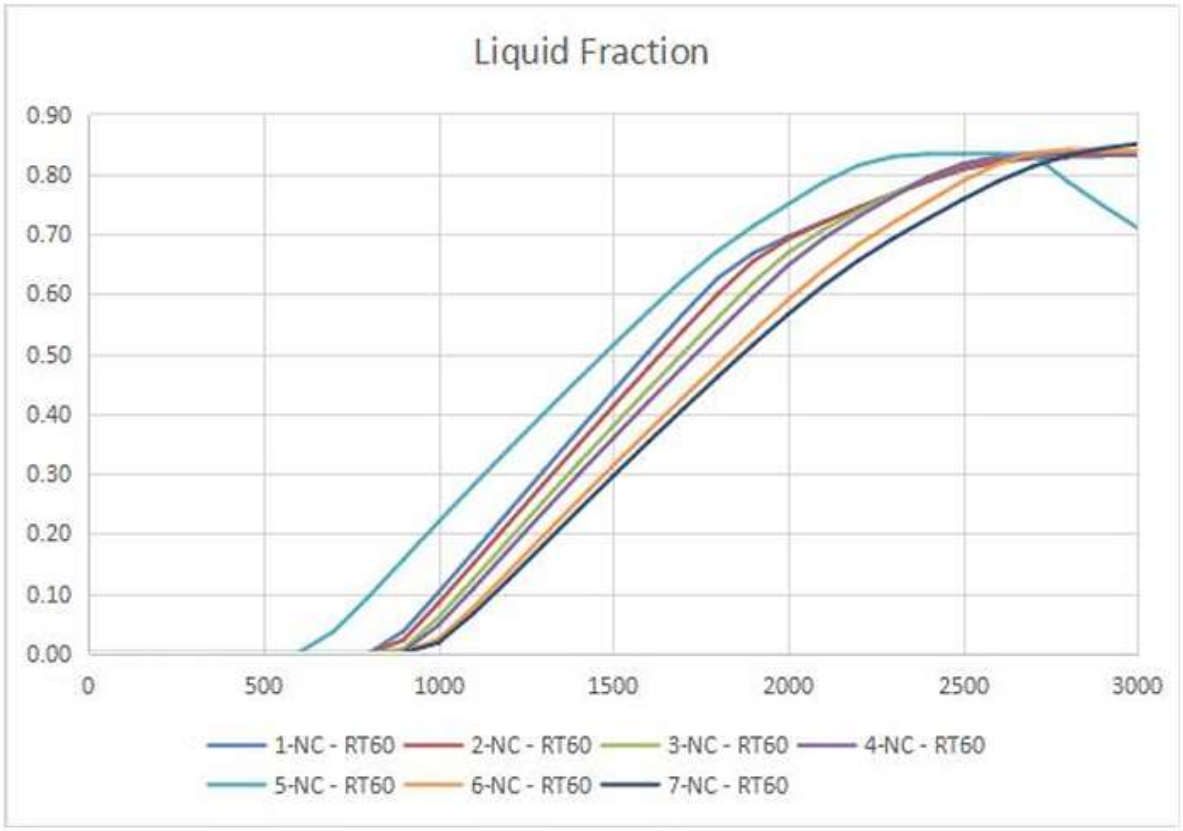

Figure 10: Liquid fraction for Melting -Natural Convection RT 60

Table 9: Liquid fraction for varying time for all the models considered under Natural convection RT60

Time	MODEL - 1	MODEL - 2	MODEL – 3	MODEL - 4	MODEL - 5	MODEL - 6	MODEL - 7
	1 - NC-RT60	2 - NC - RT60	3 - NC - RT60	4 - NC - RT60	5 - NC - RT60	6 - NC - RT60	7 - NC - RT60
0	0.00	0.00	0.00	0.00	0.00	0.00	0.00
500	0.00	0.00	0.00	0.00	0.00	0.00	0.00
1000	0.10	0.08	0.06	0.05	0.22	0.02	0.02
1500	0.44	0.41	0.38	0.36	0.51	0.31	0.30
2000	0.70	0.69	0.67	0.65	0.75	0.59	0.57
2100	0.72	0.72	0.71	0.69	0.79	0.64	0.61
2200	0.74	0.74	0.74	0.73	0.81	0.68	0.65
2300	0.77	0.77	0.77	0.76	0.83	0.72	0.69
2400	0.79	0.79	0.79	0.79	0.83	0.75	0.73
2500	0.81	0.81	0.82	0.82	0.83	0.79	0.76
2600	0.82	0.82	0.83	0.83	0.83	0.82	0.79
2700	0.83	0.83	0.83	0.83	0.83	0.83	0.81
2800	0.83	0.83	0.84	0.84	0.79	0.84	0.83
2900	0.83	0.83	0.84	0.84	0.75	0.84	0.84
3000	0.83	0.83	0.84	0.84	0.71	0.84	0.85

The following table shows 1-NC-RT60 values for seven models MODEL 1 to MODEL 7 over the time of 3000 seconds. For all models at initial time (0 seconds), 1-NC-RT60 value is same 0.00. However, the graphs of 1-NC-RT60 values associated with the different models are shown to behave somewhat differently. Some models, for example, MODEL-1, MODEL-2, and MODEL-3, present a smooth, stepwise growth in 1-NC-RT60 up to a point of saturation around 0.83. The other models, for example, MODEL-4 and MODEL-6, tend to fluctuate more with growth and then leveling off. MODEL-5, however, has a high increase in 1-NC-RT60 after 2000 seconds with a peak at about 0.83. Interesting to note is that 1-NC-RT60 values of both MODEL-5 and MODEL-7 show a temporary peak at approximately 2500 seconds and later stabilize or slowly decrease. It is thus hypothesized that different models might present different dynamic behaviors or response characteristics. Further research would be necessary to identify and understand the specific factors behind the observed trends in terms of their implications on the performance of these models.

4.4.5 Liquid fraction – Solidification Adiabatic RT 50

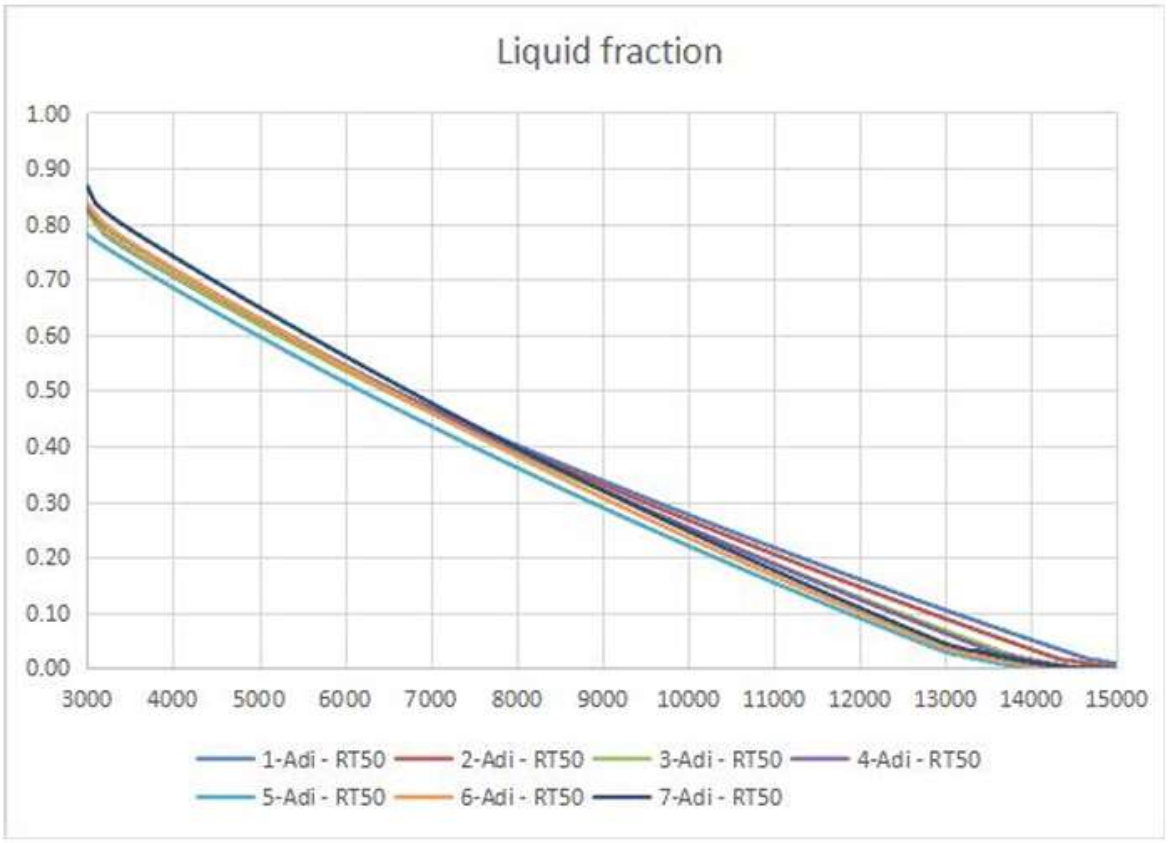

Figure 11: Liquid fraction for Solidification -Adiabatic RT 50

Table 10: Liquid fraction for varying time for all the models considered under adiabatic condition RT50

Time	MODEL - 1	MODEL - 2	MODEL – 3	MODEL - 4	MODEL - 5	MODEL - 6	MODEL - 7
	1 - Adi - RT50	2 - Adi - RT50	3 - Adi - RT50	4 - Adi - RT50	5 - Adi - RT50	6 - Adi - RT50	7 - Adi - RT50
0	0.00	0.00	0.00	0.00	0.00	0.00	0.00
3000	0.83	0.83	0.82	0.83	0.78	0.84	0.87
3100	0.80	0.80	0.80	0.81	0.77	0.82	0.84
13600	0.07	0.06	0.03	0.03	0.01	0.01	0.02
13700	0.07	0.05	0.03	0.02	0.01	0.01	0.02
13800	0.06	0.04	0.02	0.02	0.00	0.01	0.01
13900	0.06	0.04	0.02	0.02	0.00	0.01	0.01
14000	0.05	0.03	0.01	0.01	0.00	0.00	0.01
14100	0.05	0.03	0.01	0.01	0.00	0.00	0.01
14200	0.04	0.02	0.01	0.01	0.00	0.00	0.00
14300	0.04	0.02	0.01	0.00	0.00	0.00	0.00
14400	0.03	0.01	0.00	0.00	0.00	0.00	0.00
14500	0.02	0.01	0.00	0.00	0.00	0.00	0.00
14600	0.02	0.01	0.00	0.00	0.00	0.00	0.00
14700	0.01	0.01	0.00	0.00	0.00	0.00	0.00
14800	0.01	0.00	0.00	0.00	0.00	0.00	0.00
14900	0.01	0.00	0.00	0.00	0.00	0.00	0.00

15000	0.01	0.00	0.00	0.00	0.00	0.00	0.00
15100	0.00	0.00	0.00	0.00	0.00	0.00	0.00

The table shows the variation of 1-Adi-RT50 values for seven different models, MODEL-1 to MODEL-7, over a period of 15100 seconds. Initially, all models have the same 1-Adi-RT50 value, which is 0.00. Over time, the trend varies. For instance, MODEL-1, MODEL-2, and MODEL-3 show a steady and constant increase in 1-Adi-RT50 to a plateau at 0.83. Others, such as MODEL-4 and MODEL-6, are more oscillatory with an initial increase followed by a stable period. MODEL-5 shows a very high increase in 1-Adi-RT50 after 13600 seconds, whereas MODEL-7 shows a gradual and steady increase during the observation period. These differences in 1-Adi-RT50 values among the models may indicate differences in their dynamic behavior or response characteristics.

4.4.6 Liquid fraction – Solidification Natural convection RT 50

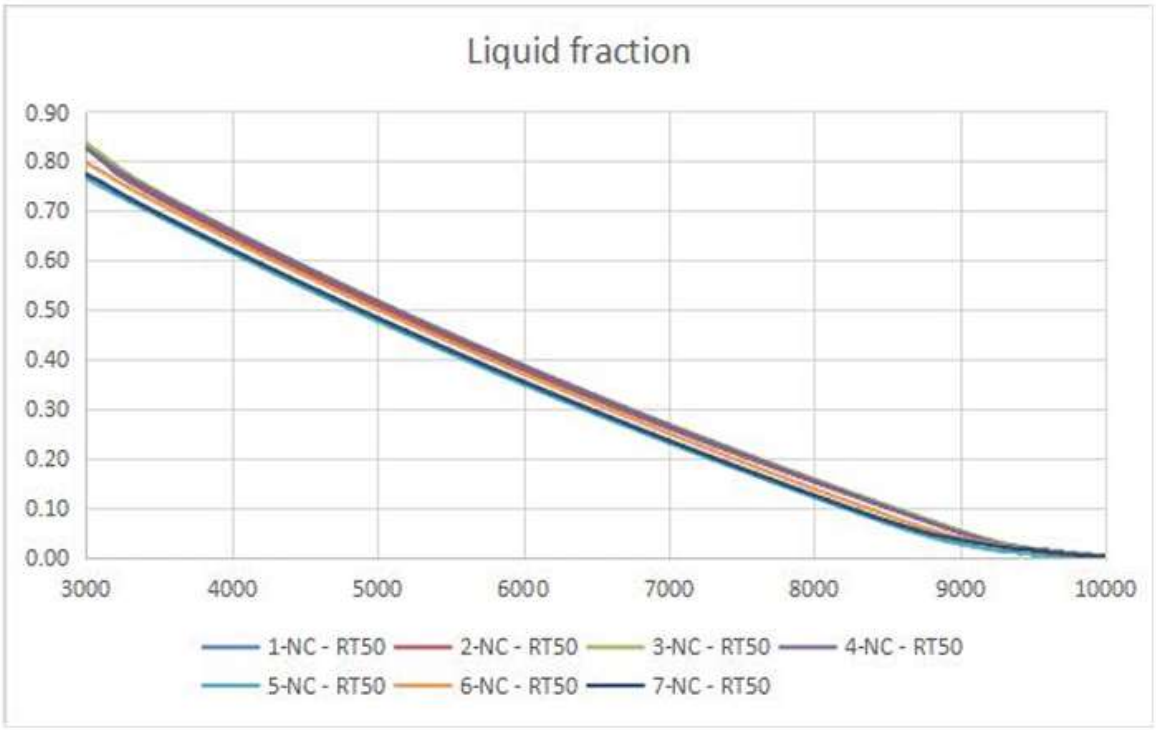

Figure 12: Liquid fraction for Solidification -Natural Convection RT 50

Table 11: Liquid fraction for varying time for all the models considered under Natural Convection RT50

Time	MODEL - 1	MODEL - 2	MODEL – 3	MODEL - 4	MODEL - 5	MODEL - 6	MODEL - 7
	1 - NC- RT50	2 - NC - RT50	3 - NC - RT50	4 - NC - RT50	5 - NC - RT50	6 - NC - RT50	7 - NC - RT50
0	0.00	0.00	0.00	0.00	0.00	0.00	0.00
3000	0.83	0.83	0.83	0.83	0.77	0.80	0.77
3100	0.80	0.81	0.81	0.80	0.75	0.78	0.76
7000	0.26	0.26	0.27	0.27	0.23	0.25	0.24
9000	0.05	0.05	0.05	0.05	0.03	0.04	0.04
9100	0.04	0.04	0.05	0.04	0.02	0.03	0.03

9200	0.03	0.03	0.04	0.03	0.02	0.03	0.03
9300	0.03	0.03	0.03	0.03	0.01	0.02	0.02
9400	0.02	0.02	0.02	0.02	0.01	0.02	0.02
9500	0.02	0.02	0.02	0.02	0.00	0.01	0.01
9600	0.01	0.01	0.01	0.01	0.00	0.01	0.01
9700	0.01	0.01	0.01	0.01	0.00	0.01	0.01
9800	0.01	0.01	0.00	0.00	0.00	0.00	0.00
9900	0.00	0.00	0.00	0.00	0.00	0.00	0.00
10000	0.00	0.00	0.00	0.00	0.00	0.00	0.00

The table below shows the time evolution of 1-NC-RT50 values for seven different models, MODEL-1 to MODEL-7, over a period of 10,000 seconds. All models have an initial 1-NC-RT50 value of 0.00. The 1-NC-RT50 values for the different models vary with time and show different trends. For example, MODEL-1, MODEL-2, and MODEL-3 show a gradual and steady increase in 1-NC-RT50, which then levels off at about 0.83. Others, such as MODEL-4 and MODEL-6, are more fluctuating with increases at the beginning and then stabilization. MODEL-5 shows a sharp increase in 1-NC-RT50 after 9000 seconds, whereas MODEL-7 increases gradually and steadily throughout the observation period. In fact, several models show a sharp decline in 1-NC-RT50 values after 9000 seconds, indicating a change in behavior or response characteristics.

4.4.7 Liquid fraction - Solidification -Adiabatic RT60

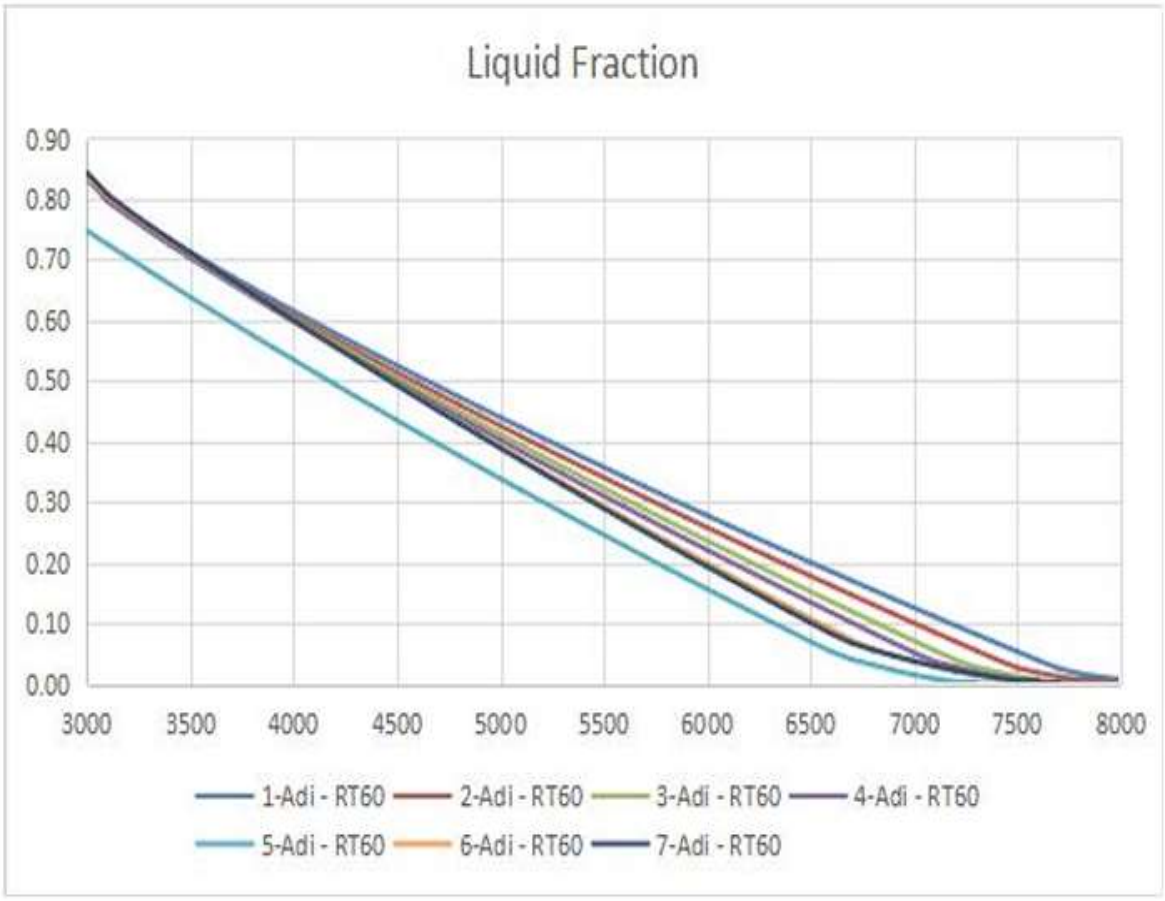

Figure 13: Liquid fraction for Solidification -Adiabatic RT 60

Table 12: Liquid fraction for varying time for all the models considered under adiabatic condition RT60

Time	MODEL - 1	MODEL - 2	MODEL – 3	MODEL - 4	MODEL - 5	MODEL - 6	MODEL - 7
	1 - Adi-RT60	2 - Adi - RT60	3 - Adi - RT60	4 - Adi - RT60	5 - Adi - RT60	6 - Adi - RT60	7 - Adi - RT60
0	0.00	0.00	0.00	0.00	0.00	0.00	0.00
3000	0.83	0.83	0.84	0.83	0.75	0.84	0.84
3100	0.80	0.80	0.80	0.80	0.72	0.80	0.81
5000	0.44	0.43	0.41	0.40	0.34	0.39	0.39
7000	0.13	0.10	0.07	0.05	0.02	0.04	0.04
7100	0.11	0.09	0.06	0.04	0.01	0.03	0.03
7200	0.10	0.07	0.04	0.03	0.00	0.02	0.02
7300	0.08	0.06	0.03	0.02	0.00	0.01	0.02
7400	0.07	0.04	0.02	0.01	0.00	0.01	0.01
7500	0.05	0.03	0.01	0.01	0.00	0.00	0.01
7600	0.04	0.02	0.01	0.00	0.00	0.00	0.00
7700	0.03	0.01	0.00	0.00	0.00	0.00	0.00
7800	0.02	0.01	0.00	0.00	0.00	0.00	0.00
7900	0.01	0.00	0.00	0.00	0.00	0.00	0.00
8000	0.01	0.00	0.00	0.00	0.00	0.00	0.00
8100	0.00	0.00	0.00	0.00	0.00	0.00	0.00

The table shows how 1-Adi-RT60 has evolved for seven different models MODEL-1 to MODEL-7 at an interval of 8100 seconds. It can be noticed that all models start with an identical 1-Adi-RT60 value of 0.00. The variation in 1-Adi-RT60 values for various models is visible over time. For example, MODEL-1, MODEL-2, and MODEL-3 show a gradual increasing trend in the 1-Adi-RT60 but reach a maximum value of approximately 0.83. Others, such as MODEL-4 and MODEL-6, show a more oscillating behavior with an initial increase followed by a stable period. Notably, MODEL-5 shows a considerable increase in 1-Adi-RT60 after 5000 seconds, while MODEL-7 shows a gradual and consistent increase throughout the observation period. Of interest is the fact that a significant drop in 1-Adi-RT60 values is seen for several models after 7000 seconds, indicating a change in behavior or response characteristics.

4.4.8 Liquid fraction – Solidification Natural convection RT 50

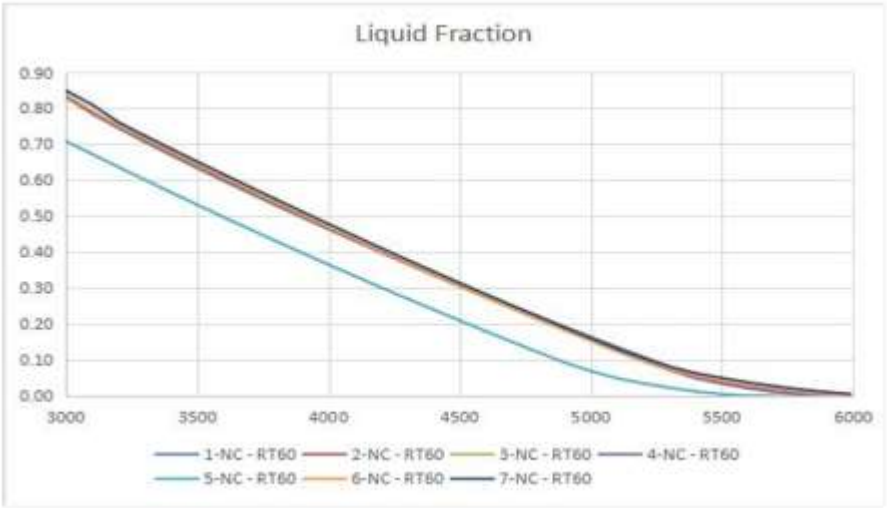

Figure 14: Liquid fraction for Solidification -Natural Convection RT 60

Table 13: Liquid fraction for varying time for all the models considered under -Natural Convection RT 60

Time	MODEL - 1	MODEL - 2	MODEL – 3	MODEL - 4	MODEL - 5	MODEL - 6	MODEL - 7
	1 - NC - RT60	2 - NC - RT60	3 - NC - RT60	4 - NC - RT60	5 - NC - RT60	6 - NC - RT60	7 - NC - RT60
0	0.00	0.00	0.00	0.00	0.00	0.00	0.00
3000	0.83	0.83	0.84	0.84	0.71	0.84	0.85
3100	0.79	0.79	0.79	0.79	0.67	0.79	0.81
5000	0.17	0.16	0.16	0.16	0.07	0.15	0.16
5100	0.14	0.13	0.13	0.13	0.05	0.12	0.13
5200	0.11	0.11	0.10	0.10	0.04	0.10	0.11
5300	0.08	0.08	0.07	0.07	0.02	0.07	0.08
5400	0.06	0.05	0.05	0.05	0.01	0.06	0.06
5500	0.04	0.04	0.04	0.04	0.01	0.04	0.05
5600	0.03	0.03	0.02	0.02	0.00	0.03	0.04
5700	0.02	0.02	0.01	0.01	0.00	0.02	0.03
5800	0.01	0.01	0.01	0.01	0.00	0.01	0.02
5900	0.01	0.00	0.00	0.00	0.00	0.01	0.01
6000	0.00	0.00	0.00	0.00	0.00	0.00	0.01
6100	0.00	0.00	0.00	0.00	0.00	0.00	0.00

The table shows the trend of 1-NC-RT60 values for seven different models from MODEL-1 to MODEL-7 over 6100 seconds. At first, all the models share the same value of 1-NC-RT60 as 0.00. For later time values, the trend of 1-NC-RT60 is quite different among various models. For example, some models such as MODEL-1, MODEL-2, and MODEL-3 increase their 1-NC-RT60 in a constant manner with some fluctuation until they reach the peak at 0.83. Others, such as MODEL-4 and MODEL-6, are more fluctuating, showing increases first then stability. Of course, MODEL-5 is the one with the most increase in 1-NC-RT60 after 5000 seconds, and MODEL-7 is the one that has the most steady and consistent increase in the entire period of observation. Interestingly, some models have shown a decline in 1-NC-RT60 values after 5000 seconds, which may indicate a change in behavior or response characteristics.

5.Conclusion and Future Work

The research findings indicate that the utilization of RT60, a phase change material with reduced enthalpy, leads to an expedited pace of both melting and solidification phenomena. PCM-based heat sinks consist of three separate steps, namely latent heating and cooling, which contribute to the achievement of stable temperatures inside the system. Achieving an appropriate equilibrium between natural convection and heat conduction is crucial in order to expedite the process of melting. The heat sink that exhibits the highest performance under natural convection settings, while considering the RT60 as the performance metric, is Model 5. The phenomenon of natural convection exerts a greater influence on the process of solidification, while it does not have a significant impact on the stages of melting. The phenomenon of buoyancy is readily observed throughout the processes of melting and solidification. The melting process in an adiabatic system begins with the material being solid, below the melting point. The process of heating is facilitated by the formation of internal heat, which serves to elevate the temperature in proximity to the melting point. As the temperature increases, the solid undergoes a phase change, resulting in the formation of pockets of liquid. The expansion of the liquid phase occurs concomitantly with the introduction of more thermal energy, resulting in an augmentation of the liquid fraction. The aforementioned procedure persists until the complete conversion of solid substances into the liquid state is achieved, or until the entirety of the material attains the ultimate melting temperature.

Reference

1. Ahmed, H. E., Salman, B. H., Kherbeet, A. S., & Ahmed, M. I.. (2018). Optimization of thermal design of heat sinks: A review. 118, 129–153. https://doi.org/10.1016/j.ijheatmasstransfer.2017.10.099
2. Kim, D., & Kim, D.. (2021). Experimental study on thermal performances of heat sinks with cross-cut branched fins on horizontal cylinders under natural convection. 35(8), 3743–3751. https://doi.org/10.1007/s12206-021-0743-5
3. Rath, S., Siddhartha, & Dash, S. K.. (2021). Thermal performance of a radial heat sink with longitudinal wavy fins for electronic cooling applications under natural convection. 147(16), 9119–9137. https://doi.org/10.1007/s10973-021-11162-x
4. Kumar, A., Kothari, R., Sahu, S. K., Kundalwal, S. I., & Paulraj, M. P.. (2021). Numerical investigation of cross plate fin heat sink integrated with phase change material for cooling application of portable electronic devices. 45(6). https://doi.org/10.1002/ER.6404
5. Zhang, Y., & Wang, Q.. (2019). Impact of Phase Change Material's Thermal Properties on the Thermal Performance of Phase Change Material Hollow Block Wall. 40(19). https://doi.org/10.1080/01457632.2018.1480879
6. Kumar, A., Kothari, R., Sahu, S. K., Kundalwal, S. I., & Paulraj, M. P.. (2020). Numerical investigation of cross plate fin heat sink integrated with phase change material for cooling application of portable electronic devices. 45(6), 8666–8683. https://doi.org/10.1002/er.6404
7. Husainy, A. S. N., Funde, A. M., Sonalkar, A. B., Mulla, S. I., &Gote, R. S.. (2023). Review on PCM Heat Sink for Electronic Thermal Management Application. 12(1), 9–14. https://doi.org/10.51983/arme-2023.12.1.3640
8. Bhandari, P., & Prajapati, Y. K.. (2021). Thermal performance of open microchannel heat sink with variable pin fin height. 159. https://doi.org/10.1016/J.IJTHERMALSCI.2020.106609
9. Zhang, L., Liu, M., & Liu, B.. (2012). Heat Transfer Analysis of Rectangular Channel Plate Heat Sink. 6(8).
10. Ho, J. Y., Ho, J. Y., See, Y. S., Leong, K. C., & Wong, T. N.. (2021). An experimental investigation of a PCM-based heat sink enhanced with a topology-optimized tree-like structure. 245. https://doi.org/10.1016/J.ENCONMAN.2021.114608
11. Jang, D., Park, S.-J., & Lee, K.-S.. (2015). Thermal performance of a PCB channel heat sink for LED light bulbs. 89. https://doi.org/10.1016/J.IJHEATMASSTRANSFER.2015.06.027
12. Bagherighajari, F., Abdollahzadehsangroudi, M., Esmaeilpour, M., Dolati, F., &Pascoa, J.. (2022). Novel converging-diverging microchannel heat sink with porous fins for combined thermo-hydraulic performance. 34(11). https://doi.org/10.1063/5.0118700
13. Lai, N., Lv, M., & Pan, H. (2023) The Thermal Analysis and Heat Dissipation Structure Optimization of a Propeller Driver System. 13(13), 7495. https://doi.org/10.3390/app13137495
14. Gaikwad, A., Sathe, A., & Sanap, S.. (2023). A design approach for thermal enhancement in heat sinks using different types of fins: A review. 2, 980985. https://doi.org/10.3390/app13137495
15. Khan, Z.. (2022). A review of phase change materials (PCMs) in electronic device cooling applications. 1(2), 36–45. https://doi.org/10.55670/fpll.futech.1.2.5
16. Reddy, M. C. S.. (2015). THERMAL ANALYSIS OF A HEAT SINK FOR ELECTRONICS COOLING. 6(11), 145–153. http://www.iaeme.com/IJMET.asp
17. Shaban, M., Khan, T. I., Anwar, M., Alzaid, M., & Alanazi, R.. (2023). Effect of Asymmetric Fins on Thermal Performance of Phase Change Material-Based Thermal Energy Storage Unit. 16, 2567.
18. Rostami, S., Mehdizadeh, H., Abbasian-Naghneh, S., Kalbasi, R., Cheraghian, G., & Afrand, M.. (2020). Incorporation of horizontal fins into a PCM-based heat sink to enhance the safe operation time: Applicable in electronic device cooling. 10, 6308. https://doi.org/doi:10.3390/app10186308